






OPEN ACCESS

Original research

# *GSN* gene frameshift mutations in Alzheimer's disease

Yaling Jiang,<sup>1</sup> Meidan Wan,<sup>1</sup> XueWen Xiao,<sup>1</sup> Zhuojie Lin,<sup>1</sup> Xixi Liu,<sup>1</sup> Yafang Zhou,<sup>2,3,4,5,6</sup> Xinxin Liao,<sup>2,3,4,5,6</sup> Jingyi Lin,<sup>3</sup> Hui Zhou,<sup>1</sup> Lu Zhou,<sup>1</sup> Ling Weng,<sup>1</sup> Junling Wang ,<sup>1,2,3,4,5</sup> Jifeng Guo ,<sup>1,2,3,4,5</sup> Hong Jiang ,<sup>1,2,4,5</sup> Zhuohua Zhang,<sup>7</sup> Kun Xia,<sup>8</sup> Jiada Li,<sup>8</sup> Beisha Tang,<sup>1,2,3,4,5</sup> Bin Jiao,<sup>1,2,3,4,5</sup> Lu Shen ,<sup>1,2,3,4,5,9</sup>

► Additional supplemental material is published online only. To view, please visit the journal online (<http://dx.doi.org/10.1136/jnnp-2022-330465>).

For numbered affiliations see end of article.

**Correspondence to**

Dr Lu Shen and Dr Bin Jiao, Department of Neurology, Xiangya Hospital Central South University, Changsha, Hunan, China; [shenlu@csu.edu.cn](mailto:shenlu@csu.edu.cn), [jiaobin@csu.edu.cn](mailto:jiaobin@csu.edu.cn)

Received 25 September 2022  
Accepted 28 December 2022  
Published Online First 17 January 2023

**ABSTRACT**

**Background** The pathogenic missense mutations of the gelsolin (*GSN*) gene lead to familial amyloidosis of the Finnish type (FAF); however, our previous study identified *GSN* frameshift mutations existed in patients with Alzheimer's disease (AD). The *GSN* genotype–phenotype heterogeneity and the role of *GSN* frameshift mutations in patients with AD are unclear.

**Method** In total, 1192 patients with AD and 1403 controls were screened through whole genome sequencing, and 884 patients with AD were enrolled for validation. Effects of *GSN* mutations were evaluated in vitro. *GSN*, A $\beta$ 42, A $\beta$ 40 and A $\beta$ 42/40 were detected in both plasma and cerebrospinal fluid (CSF).

**Results** Six patients with AD with *GSN* P3fs and K346fs mutations (0.50%, 6/1192) were identified, who were diagnosed with AD but not FAF. In addition, 13 patients with AD with *GSN* frameshift mutations were found in the validation cohort (1.47%, 13/884). Further in vitro experiments showed that both K346fs and P3fs mutations led to the *GSN* loss of function in inhibiting A $\beta$ -induced toxicity. Moreover, a higher level of plasma ( $p=0.001$ ) and CSF ( $p=0.005$ ) *GSN* was observed in AD cases than controls, and a positive correlation was found between the CSF *GSN* and CSF A $\beta$ 42 ( $r=0.289$ ,  $p=0.009$ ). Besides, the *GSN* level was initially increasing and then decreasing with the disease course and cognitive decline.

**Conclusions** *GSN* frameshift mutations may be associated with AD. An increase in plasma *GSN* is probably a compensatory reaction in AD, which is a potential biomarker for early AD.

**INTRODUCTION**

Alzheimer's disease (AD) is a neurodegenerative disease that causes a progressive decline in memory and cognitive function.<sup>1</sup> Although the majorities of AD cases occur on a sporadic basis, mutations in three genes, including amyloid precursor protein (*APP*), presenilin 1 (*PSEN1*) and presenilin 2 (*PSEN2*), can lead to rare familial AD. Its symptoms occur earlier than sporadic AD, usually between 30 years and 50 years of age. However, late-onset AD, more than 65 years of age onset, may be motivated by a complex interaction between genetic and environmental factors.<sup>2</sup> The current theories of AD pathogenesis are  $\beta$ -amyloid (A $\beta$ ) plaques and neurofibrillary tangles, with consequences of microglial activation, synaptic deficiency and neuronal loss.<sup>1,3</sup>

**WHAT IS ALREADY KNOWN ON THIS TOPIC**

⇒ Amyloid protein deposition is a common mechanism of hereditary amyloidosis and Alzheimer's disease (AD). Mutations of the gelsolin (*GSN*) gene can lead to familial amyloidosis of the Finnish type (FAF), but the relationship is unclear between these genes and AD.

**WHAT THIS STUDY ADDS**

⇒ We identified the *GSN* genotype–phenotype heterogeneity that *GSN* frameshift mutations causing AD but not FAF and clarified the role of *GSN* gene in the pathogenesis of AD.

**HOW THIS STUDY MIGHT AFFECT RESEARCH, PRACTICE OR POLICY**

⇒ We identified a potential risk factor for AD, and *GSN* mutations may explain a small portion of AD.

The *GSN* gene, encoding gelsolin (*GSN*), is a calcium-regulated actin regulatory protein that is recognised to be functionally involved in inflammation, cell movement, apoptosis and cancer development.<sup>4</sup> The *GSN* is suggested to be implicated in AD, based on the previous findings that *GSN* can bind A $\beta$ , inhibit A $\beta$ -induced toxicity, and protect cells from apoptosis and reactive oxygen species (ROS).<sup>4–6</sup> The well-known pathogenic missense mutations of the *GSN* gene have been reported to be associated with familial amyloidosis of the Finnish type (FAF), which mainly manifests as corneal lattice dystrophy, cranial neuropathy, peripheral neuropathy and cutis laxa.<sup>7</sup> Recently, we reported patients with *GSN* frameshift mutations were characterised by the typical AD phenotype.<sup>8</sup> Among the five patients with AD (cases 1–5) with *GSN* frameshift mutations, unfortunately, only the patient with the K346fs mutation (case 1) accepted Pittsburgh compound ([<sup>11</sup>C]PIB)positron emission tomography (PET) examination and was confirmed to have cerebral A $\beta$  deposition; however, no patient agreed to undergo skin biopsy, which is of great help in differentiating the diagnosis of FAF.<sup>8</sup> Thus, we could not completely determine whether these patients with frameshift mutations had FAF. Therefore, the heterogeneity of genotype–phenotype in the *GSN* gene, as well as the role of the *GSN* frameshift mutation in the pathogenesis of AD, is still unclear.

 Check for updates

© Author(s) (or their employer(s)) 2023. Re-use permitted under CC BY-NC. No commercial re-use. See rights and permissions. Published by BMJ.

**To cite:** Jiang Y, Wan M, Xiao X, et al. *J Neurol Neurosurg Psychiatry* 2023;**94**:436–447.

**Table 1** Demographic information of the enrolled gene sequencing and plasma GSN detection participants

	Gene sequencing cohort			Plasma GSN detection cohort		
	NC	AD	P value	NC	AD	P value
Numbers	1403	1192		103	124	
Age (years)	67.78±7.15	63.93±11.18	0.000****	65.99±7.89	65.19±9.27	0.487
Gender, n (%)						
Male	664 (47.3)	475 (39.8)	0.000****	34 (33.00)	50 (40.32)	0.256
Female	739 (52.7)	717 (60.2)		69 (67.00)	74 (59.68)	
ApoE, n (%)						
APOE4 carriers	269 (19.2)	531 (44.5)	0.000****	15 (14.6%)	74 (59.68%)	0.000****
APOE4 non-carriers	1134 (80.8)	661 (55.5)		88 (85.4%)	50 (40.32%)	
MMSE	27.53±1.73	11.66±7.27	0.000****	27.81±2.08	16.08±8.02	0.000****
Plasma GSN level (pg/mL)	–	–		(1.22±0.31)×10 <sup>7</sup>	(1.40±0.43)×10 <sup>7</sup>	0.001***

\*\*\*P<0.001, \*\*\*\*P<0.0001.

AD, Alzheimer's disease; GSN, gelsolin; MMSE, Mini-Mental State Examination; NC, normal control.

In the present study, we found 0.50% of AD cases carrying the GSN frameshift mutations, who were not accompanied by other dementia-related gene mutations through whole genome sequencing (WGS) technology. The diagnosis of AD, but not FAF, was confirmed by [<sup>11</sup>C] PiB-PET and skin biopsy. Besides, the GSN loss-of-function effect of frameshift mutations was verified through in vitro experiments (Aβ-induced toxicity and apoptotic tests) and the detection of decreased GSN mRNA and GSN level in plasma. Moreover, the GSN level in plasma was increasing in sporadic AD cases compared with controls, indicating that the increasing plasma GSN may be a potential biomarker for AD. This work first claimed that the frameshift mutations in the GSN gene were associated with sporadic AD through its loss-of-function mechanisms.

## MATERIALS AND METHODS

### Subjects

We enrolled a total of 1192 patients with AD from the Department of Neurology, Xiangya Hospital (table 1). All patients were diagnosed as AD according to the 2011 National Institute of Ageing and Alzheimer's Association (NIA-AA) criteria for probable AD.<sup>9</sup> All participants were sequenced through WGS to identify the GSN mutational spectrum, and meanwhile, other dementia-related gene causative mutations were excluded. The GSN mutations were further validated in two validation cohorts of the Cognitive Impairment Multicenter Database and Collaborative Network in China (CI-MDCNC), as well as the Alzheimer's Disease Sequencing Project (ADSP)<sup>10–12</sup> (online supplemental methods). The CI-MDCNC includes 884 patients with probable AD who underwent gene-targeted sequencing (online supplemental methods). Besides, 1403 cognitively unimpaired controls were enrolled from Xiangya Hospital Health Management Centre (table 1).

Additionally, 124 patients with AD and 103 cognitively unimpaired controls, which were sex-matched and age-matched, were recruited for GSN detection in plasma samples. A total of 82 patients with AD and 59 controls further underwent cerebrospinal fluid (CSF) GSN detection. Meanwhile, 82 patients with AD underwent CSF AD biomarker examinations, including Aβ<sub>40</sub>, Aβ<sub>42</sub>, Aβ<sub>42/40</sub>, t-tau and p-tau, which met the 2018 NIA-AA criteria<sup>13</sup> for the framework diagnosis of AD for A+T+n+classification (online supplemental methods).

### WGS and data analysis

The formalin-fixed paraffin-embedded (FFPE) DNA was extracted using the MagPure FFPE DNA LQ Kit following the

manufacturer's instruction. The sample's concentration was detected by Qubit fluorometer. The integrity and purification of samples were detected by agarose gel electrophoresis. One nanogram and more FFPE DNA were randomly fragmented by Covaris. Fragmented DNAs were tested by Agilent 2100 and purified by the Agencourt AMPure XP kit. The selected fragments were end-repair and 3' adenylated; at the same time, the adapters were ligated to the ends of these 3' adenylated fragments. These fragments were amplified with KAPA HiFi HotStart DNA polymerase, and the PCR products were purified with the Agencourt AMPure XP kit. The library was qualified by the Agilent 2100 Bioanalyzer and ABI StepOne-Plus real-time PCR (RT-PCR) system. The qualified libraries were sequenced pair end on the Hiseq4000/Xten/Novaseq system (BGI, Shenzhen, China). We used Genome Analysis Toolkit software to detect (Single Nucleotide Variants) SNVs and indels. All SNVs and indels were filtered and estimated via multiple databases, including Genome Aggregation Database and Exome Aggregation Consortium. Common variants and rare variants were classified according to minor allele frequencies (MAFs; common variants: MAF ≥0.01, rare variants: MAF <0.01).<sup>14</sup>

### Real-time PCR

The blood samples of subjects were freshly collected. Total RNA was extracted using *TransZol* Up Plus RNA Kit (catalogue number 315–150; GeneAll, Korea), and cDNA was synthesised from 1 µg of total RNA by using the NovoScept Plus All-in-One First Strand cDNA Synthesis Kit (catalogue number E047; Novoprotein, China). For PCR, the cDNA was amplified with 2× MPCR OPTI Mix (catalogue number B45012; Bimake, USA) in a T100 Thermal Cycler (Bio-Rad, USA). The primers for the two GSN frameshift mutations are shown in online supplemental figure S1A. Next, the PCR products were subjected to agarose gel electrophoresis. For RT-PCR, the cDNA was amplified with 2× SYBR Green qPCR Master Mix (catalogue number B21202, Bimake) using FTC-3000 RT-PCR system (Funglyn Biotech, Canada). The relative standard curve method (2<sup>-ΔΔC<sub>t</sub></sup>) was used to determine the relative gene expression, and *GAPDH* was used as a housekeeping gene for internal normalisation. The PCR primers were as follows: GSN: forward, 5'-AGCTGGCCAAGCTCTACAAG-3', and reverse, 5'-TTCCTCTCCTCCGTGTTTGC-3'; *GAPDH*: forward, 5'-AGTAAAAGCAGCCCTGGTGA-3', and reverse, 5'-TCGACAGTCAGCCGCATCT-3'.

### Plasma GSN detection

The venous blood samples were collected using standard venipuncture protocols after an overnight fast. Then, plasma was collected in 30 min by centrifugation at 1000 rpm and 4°C for 10 min. The plasma GSN level was detected by GSN ELISA kit (catalogue number ab270215; Abcam, USA). All procedures were performed in accordance with the manufacturer's instructions.

### CSF GSN and AD biomarker detection

The CSF sample was collected according to international guidelines.<sup>15</sup> Samples were centrifuged at 2000×g and 4°C for 10 min and stored at -80°C. The CSF GSN level was detected by GSN ELISA kit (catalogue number ab270215, Abcam). All procedures were performed in accordance with the manufacturer's instructions.

All CSF AD biomarkers (Aβ42, Aβ40, t-tau and p-tau) were measured using ELISA kits (catalogue numbers EQ 6511-9601, EQ 6521-9601, EQ 6591-9601, EQ 6531-9601; EURO-IMMUN, Germany), and the detection was performed by experienced technicians in strict accordance with the instructions of the manufacturer within 1 week of sample collection.

### Cell culture

The SH-SY5Y cells (catalogue number ZQ0050; Zhong Qiao Xin Zhou Biotechnology, Shanghai, China) were cultured in high glucose Dulbecco's Modified Eagle's Medium (DMEM) (catalogue number C11995500BT, Gibco) supplemented with 10% Fetal Bovine Serum (FBS) and 1% PS at 37°C and 5% CO<sub>2</sub> in a humidified atmosphere. The SH-SY5Y-APPswe stable cell lines were constructed by lentiviral infection with the APPswe mutation (specials: Homo sapiens, NM\_201414.3: c.1785G>Cp.K595N; c.1786A>Cp.M595L).<sup>16</sup> The control cell lines were transfected with empty lentivirus (EV). Western blot analysis of APP was performed to demonstrate the successful construction of APPswe cell lines (online supplemental figure S2).

### Transfection of GSN plasmids and detection of the levels of Aβ42 and Aβ40

A total of 5×10<sup>4</sup> cells (SH-SY5Y-APPswe and SH-SY5Y-EV) were sealed on a 24-well plate with 500 μL of medium. After 24 hours, cells were transfected with GSN plasmids using Lipofectamine 3000 Transfection Reagent (catalogue number L3000015, Thermo). The GSN plasmids with 3× flagtag were cloned into the eukaryotic expression pIRES2-DsRed2. The ratio of Lipo3000/DNA was 1.5 μL/μg. Six hours later, the culture medium was changed to DMEM with 10% FBS. Then, the cell culture was collected to detect Aβ levels by ELISA, and cells were calculated for apoptosis by Hoechst staining<sup>17</sup> after 48 hours. The concentrations of Aβ42 and Aβ40 were measured using commercial ELISA kits (catalogue numbers DAB142 and DAB140B; R&D, USA). All procedures were performed in accordance with the manufacturer's instructions.

### Hoechst staining and apoptosis analysis

Cells were stained with Hoechst 33342 (catalogue number 40732ES03; Yeasen, China) after fixation according to the manufacturer's protocol. A fluorescence microscope (Carl Zeiss Axio Imager 2; Carl Zeiss, Germany) was used to obtain the image. As the nuclei of apoptotic cells were concentrated, apoptotic cells were observed to have high fluorescence intensity by Hoechst staining and were noted as Hoechst-positive cells.<sup>17</sup> The percentage of Hoechst-positive cells was analysed by ImageJ software.

### ROS streaming detection

A total of 3×10<sup>5</sup> cells (SH-SY5Y-APPswe and SH-SY5Y-EV) were sealed on a six-well plate with 2 mL of medium. The same procedures were performed to transfect GSN plasmids as mentioned previously. The cells were collected for ROS streaming detection using a Cell Metre Fluorimetric Intracellular Total ROS Activity Assay Kit Brite 670 nm (catalogue number 22903; AAT Bioquest, USA). All procedures were performed in accordance with the manufacturer's instruction.

### CCK8 analysis

A total of 5×10<sup>4</sup> SH-SY5Y cells were sealed on a 24-well plate with 500 μL of medium. After 24 hours, the culture media were changed to media supplemented with different concentration gradients of Aβ40 (0, 1, 5, 10 and 20 μM). The CCK8 Kit (catalogue number ab228554, Abcam) was applied to cells after 48 hours to evaluate the toxicity of the Aβ40 according to the manufacturer's instructions.

### Live/dead cell staining

The SH-SY5Y cells were sealed on a 24-well plate with 500 μL of medium. Twenty-four hours later, the cells were transfected with GSN plasmids, and the procedures were the same as mentioned previously. After 6 hours, the culture medium was changed to DMEM with 10% FBS and 5 μM Aβ40. The treated cells were washed twice with assay buffer and stained with calcein-AM (4 μM) and PI solution (9 μM) using the Calcein-acetoxymethyl ester (AM)/propidium iodide (PI) Double Stain Kit (catalogue number 40747ES76, Yeasen). After incubation for 30 min at 37°C, the cells were washed and photographed using a fluorescence microscope. The percentages of dead cells (calcein-AM<sup>-</sup>PI<sup>+</sup>) were calculated.<sup>18</sup>

### Western blot analyses

Cells were collected and resuspended in RIPA lysis buffer (catalogue number P0013B; Beyotime, China) containing a protease and phosphatase inhibitor mixture. Cell suspensions were lysed on ice for 30 min, sonicated and centrifuged at 13 000 rpm for 10 min at 4°C. Briefly, protein concentrations were estimated using BCA Kit (catalogue number 70-PQ0012; MULTI SCIENCES, China). Lysates were separated on 10% or 12% sodium dodecyl sulfate-polyacrylamide electrophoresis gels (catalogue number P1200; Solarbio, China). After separation, the protein was transferred to a Poly Vinylidene Fluoride (PVDF) membrane (catalogue numbers IPVH00010 and ISEQ00010; Millipore, USA), and non-specific binding sites were blocked by treatment with commercial western blocking buffer (catalogue number SW3010, Solarbio) followed by antibody incubation: flag tag (1:1000, catalogue number A00187; GenScript, China), APP (1:1000, catalogue number ab32136; Abcam) and β-actin (1: 1000, catalogue number O10313; TransGen, China). Horse radish peroxidase (HRP)-conjugated secondary antibodies (1: 5000, Solarbio) were used. Western blot images were captured by the ChemiDoc™ XRS+ with Image Lab Software (Bio-Rad).

#### Statistical analysis

All measurement data are presented as mean±SD. Unpaired, two-tailed Student's t-test was used to analyse the differences between two groups. Sex and APOE phenotype were analysed by χ<sup>2</sup> test. Statistical analysis of multiple-group comparisons was performed by one-way analysis of variance. The correlation analyses were adopted Pearson or Spearman correlation analysis. The significance of gene enrichment was measured by Fisher's



**Table 2** Rare and damaging variants of the *GSN* gene in our cohort

AA change	SNP	Mutation type	gnomAD_ exome _ALL	gnomAD_ exome _EAS	ExAC_ ALL	ExAC_ EAS	ReVe	Functional predictions: pathogenic (total)	Patients	Controls
Frameshift mutations										
Exon1:c.8_35del:p.P3fs	rs764841269	Frameshift	0	0	0	0	NA	NA	5	0
Exon7:c.1036delA:p.K346fs	NA	Frameshift	NA	NA	NA	NA	NA	NA	1	0
Carriers (n)									6	0
Frequency (%)									0.50% (6/1192)	0.00% (0/1403)
P value									0.025*	
Missense mutations										
Exon2:c.215G>A:p.R72H	rs766916675	Missense	1.62E-05	0.0002	8.24E-06	0	0.780	16 (20)	1	0
Exon3:c.402G>C:p.Q134H	NA	Missense	NA	NA	NA	NA	0.708	15 (20)	1	0
Exon3:c.461C>T:p.S154L	rs767484600	Missense	1.63E-05	0.0002	1.66E-05	0.0002	0.762	16 (20)	0	2
Exon4:c.563G>T:p.R188I	rs761093581	Missense	3.25E-05	0.0005	4.13E-05	0.0006	0.763	16 (20)	1	0
Exon6:c.902A>G:p.Y301C	rs758752620	Missense	4.08E-06	5.80E-05	8.30E-06	0.0001	0.737	16 (20)	2	0
Exon10:c.1357G>A:p.E453K	rs368079865	Missense	4.47E-05	0	6.61E-05	0	0.740	16 (20)	0	2
Exon12:c.1574G>A:p.R525H	rs142828669	Missense	0.0002	0	0.0002	0	0.751	15(20)	1	0
Exon12:c.1691G>A:p.R564H	rs148410442	Missense	6.09E-05	0.0003	9.01E-05	0.0008	0.767	16(20)	0	1
Exon12:c.1730G>T:p.R577L	rs528604896	Missense	7.80E-05	0.0011	6.75E-05	0.001	0.724	16(20)	3	3
Carriers (n)									9	8
Frequency (%)									0.76% (9/1192)	0.57% (8/1403)
P value									0.561	
The silico tools for predicting variants were (1) SIFT ( <a href="http://sift.jcvi.org">http://sift.jcvi.org</a> ), (2) PolyPhen2-HDIV ( <a href="http://genetics.bwh.harvard.edu/pph2">http://genetics.bwh.harvard.edu/pph2</a> ), (3) PolyPhen2-HVAR ( <a href="http://genetics.bwh.harvard.edu/pph">http://genetics.bwh.harvard.edu/pph</a> ), (4) LRT ( <a href="http://www.genetics.wustl.edu/jflab/lrt_query.html">http://www.genetics.wustl.edu/jflab/lrt_query.html</a> ), (5) MutationTaster ( <a href="http://www.mutationtaster.org">http://www.mutationtaster.org</a> ), (6) MutationAssessor ( <a href="http://mutationassessor.org">http://mutationassessor.org</a> ), (7) FATHMM ( <a href="http://fathmm.biocompute.org.uk">http://fathmm.biocompute.org.uk</a> ), (8) PROVEAN ( <a href="http://provean.jcvi.org/">http://provean.jcvi.org/</a> ), (9) MCAP ( <a href="http://bejerano.stanford.edu/MCAP">http://bejerano.stanford.edu/MCAP</a> ), (10) CADD ( <a href="http://cadd.gs.washington.edu/">http://cadd.gs.washington.edu/</a> ), (11) DANN ( <a href="https://cbcl.ics.uci.edu/public_data/DANN/">https://cbcl.ics.uci.edu/public_data/DANN/</a> ), (12) Eigen ( <a href="http://www.columbia.edu/~ii2135/eigen.html">http://www.columbia.edu/~ii2135/eigen.html</a> ), (13) GenoCanyon ( <a href="http://genocanyon.med.yale.edu/">http://genocanyon.med.yale.edu/</a> ), (14) fitCons ( <a href="http://compugen.csh.edu/fitCons/">http://compugen.csh.edu/fitCons/</a> ), (15) VEST3 ( <a href="http://wiki.chasmosoftware.org">http://wiki.chasmosoftware.org</a> ), (16) MetaSVM ( <a href="https://www.ncbi.nlm.nih.gov/pubmed/25552646">https://www.ncbi.nlm.nih.gov/pubmed/25552646</a> ), (17) MetaLR ( <a href="https://www.ncbi.nlm.nih.gov/pubmed/25552646">https://www.ncbi.nlm.nih.gov/pubmed/25552646</a> ), (18) fathmm-MKL ( <a href="http://fathmm.biocompute.org.uk/">http://fathmm.biocompute.org.uk/</a> ), (19) REVEL ( <a href="https://sites.google.com/site/revelgenomics">https://sites.google.com/site/revelgenomics</a> ) and (20) ReVe ( <a href="https://pubmed.ncbi.nlm.nih.gov/30060008/">https://pubmed.ncbi.nlm.nih.gov/30060008/</a> ).										
AA, amino acid; EAS, East Asia population; ExAC, Exome Aggregation Consortium; gnomAD, Genome Aggregation Database dataset; GSN, gelsolin; NA, not available; SNP, single-nucleotide polymorphisms.										

exact test.<sup>19</sup> GraphPad Prism software V.8.0 and SPSS V.23.0 were used for the aforementioned statistical analysis.

The details of the three-dimensional (3D) model structure and the scales of global cerebral atrophy–frontal subscale (GCA-F), posterior atrophy (PA) and medial temporal lobe atrophy (MTA) are described in the online supplemental methods.

## RESULTS

### Frameshift mutations of the *GSN* gene may lead to AD *GSN* gene frameshift mutations were significantly enriched in patients with AD

The WGS was performed in the cohort including 1192 patients with AD (63.93±11.18 years) and 1403 cognitively normal controls (NCs, 67.78±7.51 years). The Mini-Mental State Examination (MMSE) scores of patients with AD (11.66±7.27) were significantly lower than those of controls (27.53±1.73,  $p=0.000$ ). All the participants were of Southern Han Chinese ancestry (table 1).

As shown in table 2, 11 rare (MAF <0.01) and damaging variants (ReVe >0.5<sup>14</sup> or Loss of function, LoF) of the *GSN* gene were identified in our cohort, including two frameshift mutations (P3fs and K346fs) and nine missense variants (R72H, Q134H, S154L, R188I, Y301C, E453K, R525H, R564H and R577L). Regarding the frameshift mutations, the frequency in patients with AD (0.50%, 6/1192) was higher than that of controls (0/1403,  $p=0.025$ ; table 2), indicating that rare damaging frameshift mutations of the *GSN* gene were enriched in patients with AD. However, we failed to identify a significant enrichment of missense variants across the *GSN* gene in patients

with AD compared with controls ( $p=0.56$ , table 2). Additionally, patients with AD carrying these variants of undetermined significance (VUS) did not develop the typical symptoms of FAF. *GSN*-R188I, *GSN*-Y301C and *GSN*-R525H were identified only in the AD cohort, not in controls, and distributed in different domains of *GSN* (table 2). The 3D structure models of these mutant proteins (R188I, Y301C and R525H) showed fewer conformational changes (online supplemental figure S3), suggesting that these variants were unlikely to lead to FAF. Thus, we selected these VUS for further in vitro experiments.

Besides, the *GSN* mutations were further validated in two cohorts from CI-MDCNC and ADSP, respectively.<sup>10–12</sup> Interestingly, three frameshift mutations (P3fs, G470fs and S552fs) were identified in the CI-MDCNC cohort, and the frequency in patients with AD (1.47%, 13/884) was higher than that of controls (0/1403,  $p<0.001$ ; online supplemental table S1). However, the *GSN* rare frameshift mutations were not observed in the ADSP cohort, indicating that the *GSN* frameshift mutations might be enriched in the Chinese populations.

### Patients with *GSN* frameshift mutations exhibited AD phenotype

There were six patients identified with *GSN* frameshift mutations, including one case with K346fs and five cases with P3fs, and no other dementia-related gene mutation was found by WGS. Among them, five patients (cases 1–5) were reported in a previous study, and one sporadic AD case (case 6) with P3fs mutation was identified in the continuous work. The case 6 patient underwent PiB-PET and skin biopsy, which supported the diagnosis of AD rather than FAF (figure 1A–C). The case 6



## Neurodegeneration

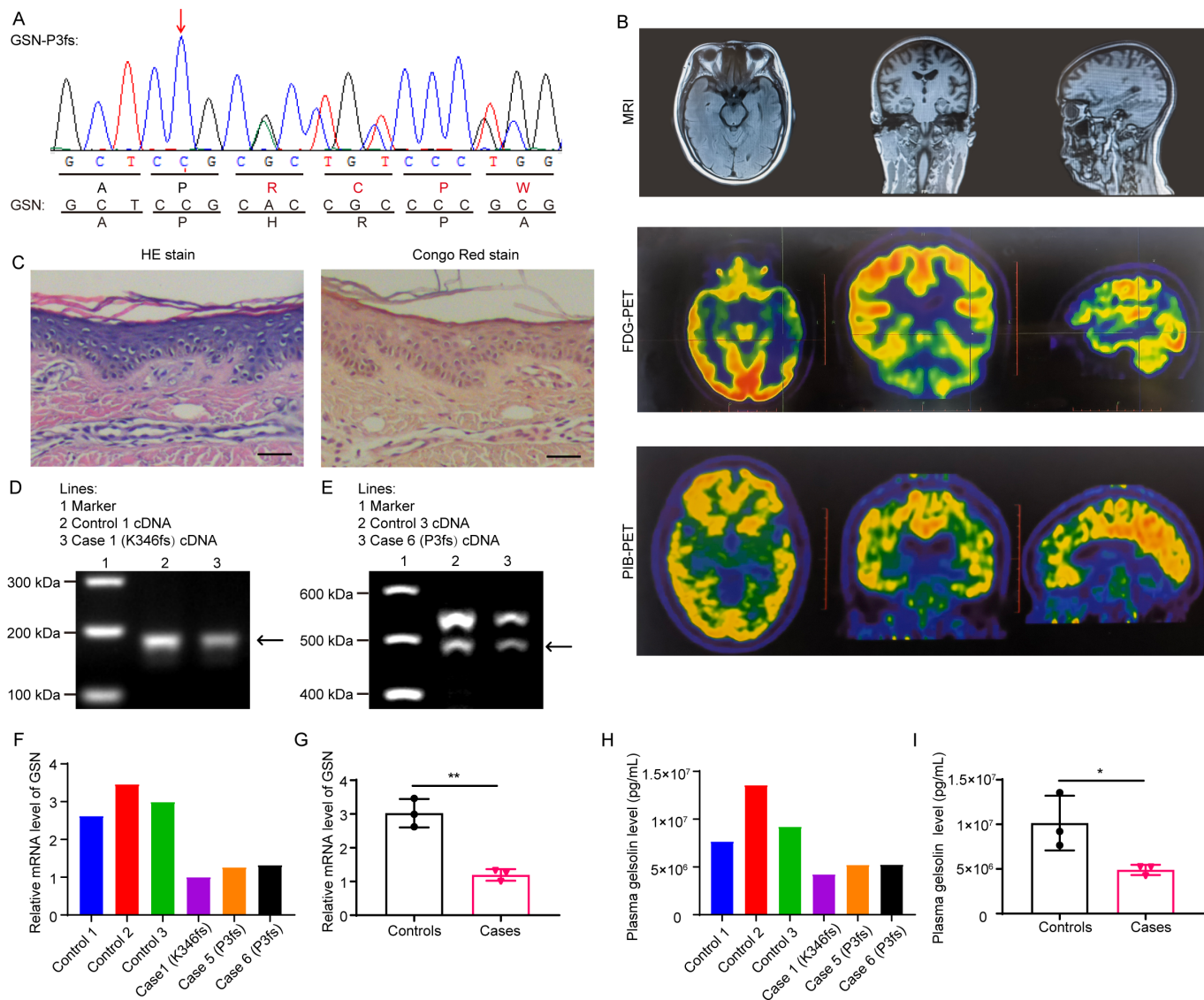


**Figure 1** Examination results of case 6 and the reduced GSN expression in patients with Alzheimer's disease with GSN frameshift mutations. (A) Nucleotide and amino acid sequences of case 6 (*GSN*:c.8\_35del:p. P3fs) and *GSN*. (B) MRI, FDG-PET and PiB-PET of case 6 with P3fs mutation. (C) The H&E staining and Congo red staining of the skin biopsy showed no amyloid deposition of case 6 with P3fs mutation. Scale bar: 50  $\mu$ m. (D) The same band between case 1 and control 1 in the electrophoresis of RT-PCR products. (E) The same band between case 6 and control 3 in the electrophoresis of RT-PCR products. (F) *GSN* mRNA expression level in case 1, cases 5 and 6, and controls 1–3 by qPCR. (G) Analysis of the data in (F). Reduced *GSN* mRNA expression level in cases compared with controls. n=3 per group. (H) Plasma GSN level in case 1, cases 5 and 6, and controls 1–3 by ELISA. (I) Analysis of the data in (H). Reduced plasma GSN level in cases compared with controls. n=3 per group. \*P<0.05, \*\*P<0.01. FDG-PET, <sup>18</sup>F-fluorodeoxyglucose positron emission tomography; GSN, gelsolin; qPCR, quantitative PCR; RT-PCR, real-time PCR.

patient, whose onset age was 52 years old, was initially presented with memory decline, manifesting as forgetting things that have just been done, and subsequently, she lost her way in the town and often called her son the wrong name. No hallucinations or delusions were observed, and there was no family history. Neuropsychological assessment showed that the MMSE and Montreal Cognitive Assessment scores were 21/30 and 13/30, respectively. Brain MRI showed mild brain atrophy (figure 1B). <sup>18</sup>F-Fluorodeoxyglucose-PET revealed decreased fluorodeoxyglucose metabolism in the bilateral-frontal and parietal lobe, and left temporal-occipital lobe; PiB-PET indicated diffuse A $\beta$  protein deposition in the bilateral cerebral cortex (figure 1B). The ophthalmological examination of the cornea was normal. The skin biopsy<sup>20 21</sup> was negative for Congo red staining (figure 1C), indicating that no amyloid or GSN was deposited in the skin.

Different from our previous work, we first confirmed that the GSN frameshift mutations can lead to AD, rather than FAF, through the PiB-PET and skin biopsy examinations together.

### GSN frameshift mutations lead to reduced expression

To study the mRNA expression of the mutant alleles, we conducted RT-PCR analysis by using peripheral lymphocytes available from the affected individuals (case 1 and cases 5 and 6). The cDNA sequences of case 1 (K346fs) and case 6 (P3fs) were the same as the genome sequencing of NCs (control 1 and control 3), respectively (figure 1D,E, and online supplemental figure S1B). In addition, the expression of *GSN* mRNA in cases carrying frameshift mutations was significantly reduced compared with that in age-matched and sex-matched controls

( $p=0.002$ ; [figure 1F,G](#)). Moreover, plasma GSN levels of cases with frameshift mutations ( $(4.89\pm 0.58)\times 10^6$  pg/mL) were decreased compared with age-matched and sex-matched NCs ( $(1.01\pm 0.31)\times 10^7$  pg/mL),  $p=0.043$ ; [figure 1H,I](#)), suggesting that these frameshift mutations might lead to the reduced expression of GSN.

### GSN frameshift mutations promote AD progression in in vitro experiments

#### GSN frameshift mutations, not missense mutations, causing the decreased GSN expression

To explore the functions of GSN mutations in pathological conditions, we first established the AD model cells by transfecting SH-SY5Y cells with the APP<sub>swe</sub> mutation (SH-SY5Y-APP<sub>swe</sub> cells), which highly expressed mutant APP proteins and generated A $\beta$ 42 deposition (online supplemental figure S2). Different GSN plasmids with the flag tag at N-terminus were transfected into SH-SY5Y-APP<sub>swe</sub> cells ([figure 2A,B](#), and [table 2](#)). Immunofluorescence results showed that SH-SY5Y-APP<sub>swe</sub> cells transfected with GSN plasmids were characterised by both GFP (green) and DsRed (red), which appeared as yellow in merged images ([figure 2A](#)). Western blot analysis of the flag tag showed the expression of GSN frameshift mutations could not detect the normal GSN size, which were almost the same in the expression of GSN wild-type or missense mutations ([figure 2B](#)).

#### GSN frameshift mutations, not missense mutations, failed to reduce A $\beta$ 42 expression

The levels of A $\beta$ 42 and A $\beta$ 40 were detected after SH-SY5Y-APP<sub>swe</sub> or SH-SY5Y-EV cells transfected with various GSN plasmids. The level of A $\beta$ 42 and the ratio of A $\beta$ 42/A $\beta$ 40 in SH-SY5Y-APP<sub>swe</sub> cells transfected with GSN-K346fs ( $42.43\pm 3.05$  pg/mL and  $0.39\pm 0.04$ , respectively) were significantly higher than those in SH-SY5Y-APP<sub>swe</sub> cells transfected with GSN-WT ( $32.91\pm 2.39$  pg/mL and  $0.27\pm 0.03$ , respectively;  $p<0.01$ ) and were similar to those in the control group (transfected with control plasmid). The level of A $\beta$ 42 in GSN-P3fs transfected group was slightly higher than that in the GSN-WT group, while no significant difference was found between the GSN-D214N, GSN-R188I, GSN-Y301C, GSN-R525H and GSN-WT groups ([figure 2C,D](#)).

#### GSN frameshift mutations, not missense mutations, causing apoptosis

The apoptotic tests, which detected by Hoechst staining, revealed that the Hoechst-positive cells of SH-SY5Y-APP<sub>swe</sub> cells transfected with GSN-K346fs ( $8.29\pm 1.22$  %) and GSN-P3fs ( $8.23\pm 0.89$  %) were more than those transfected with GSN-WT ( $4.61\pm 1.08$ %,  $p<0.0001$ ; [figure 2E,F](#)), while the Hoechst-positive cells of GSN-D214N, GSN-R188I, GSN-Y301C and GSN-R525H groups were similar to the GSN-WT group ([figure 2E,F](#)). However, streaming detection of ROS in SH-SY5Y-APP<sub>swe</sub> and SH-SY5Y-EV cells transfected with various GSN plasmids showed no difference ([figure 2G](#)).

#### GSN frameshift mutations, not missense mutations, losing the ability to inhibit the toxicity of A $\beta$ 40

The ability of different GSN mutations to inhibit the toxicity of A $\beta$ 40 was detected in SH-SY5Y cells. Toxicity analysis by CCK8 showed that the concentration of  $5\mu\text{M}$  A $\beta$ 40 was a suitable concentration for intervention ([figure 3A](#)). The SH-SY5Y cells were transfected with different GSN plasmids and treated with  $5\mu\text{M}$  A $\beta$ 40. The immunostaining of calcein-AM and propidium

iodide (PI) confirmed the higher ratio of dead cells:live cells in the GSN-K346fs ( $15.01\%\pm 3.06\%$ ,  $p<0.0001$ ) and GSN-P3fs ( $13.81\%\pm 5.09\%$ ,  $p<0.0001$ ) groups than that in the GSN-WT group ( $4.29\%\pm 1.60\%$ ; [figure 3B,C](#)), indicating that the K346fs and P3fs mutations lost the ability to inhibit the toxicity of A $\beta$ . The ratio of dead cells:live cells in the GSN-D214N, GSN-R188I, GSN-Y301C and GSN-R525H groups was similar to that in the GSN-WT group ([figure 3B,C](#)).

### GSN levels in patients with sporadic AD

#### Higher plasma and CSF GSN levels were observed in patients with sporadic AD

To explore whether the level of plasma GSN was a potential biomarker for AD, a total of 124 patients with AD without GSN mutations ( $65.19\pm 9.27$  years) and 103 cognitively unimpaired control subjects ( $65.99\pm 7.89$  years), which were sex-matched and age-matched, underwent plasma GSN detection ([table 1](#)). The plasma GSN level was much higher in patients with AD ( $(1.40\pm 0.43)\times 10^7$  pg/mL) than that in controls ( $(1.22\pm 0.31)\times 10^7$  pg/mL,  $p=0.001$ ; [figure 4A](#)).

Then, 82 A+T+n+ patients with AD and 59 cognitively unimpaired control subjects, which were sex- and age-matched, underwent both plasma and CSF GSN detection. The CSF GSN level was much higher in patients with AD ( $(6.57\pm 2.54)\times 10^5$  pg/mL) than that in controls ( $(5.21\pm 3.14)\times 10^5$  pg/mL,  $p=0.005$ ; [figure 4B](#)). Besides, a positive correlation between the CSF GSN and plasma GSN was found in patients with AD ( $r=0.234$ ,  $p=0.017$ ; [figure 4C](#)), suggesting that the plasma GSN could reflect the level of GSN in the CSF of patients with AD.

#### Decreased plasma GSN levels were observed in patients with AD with GSN frameshift mutations, rather than missense mutations

The plasma GSN level in patients with AD with GSN frameshift mutations ( $(4.93\pm 1.79)\times 10^6$  pg/mL) exhibited extremely lower than that in controls, patients with AD without GSN mutations or patients with AD with GSN missense mutation ( $p<0.05$ ,  $p<0.001$  and  $p<0.01$ , respectively; [figure 4A](#)). However, patients with AD with GSN missense mutations (R188I, Y301C, and R525H) showed similar plasma GSN levels with controls or patients with AD without GSN mutations ( $p>0.05$ ; [figure 4A](#)). Overall, it indicated that the reduced plasma GSN level was only observed in patients with AD with GSN frameshift mutations.

#### Plasma GSN levels were correlated with cognitive state in AD patients

To explore the relationship between the plasma GSN level and cognitive state, the plasma GSN levels were compared between groups of different Clinical Dementia Rating (CDR) scores. The plasma GSN level was initially increased in the groups of CDR score=0.5 ~ 2, and then reduced in the group of CDR score=3 ([figure 4D](#)). Therefore, patients with AD with mild cognitive impairment might have a higher plasma GSN level, while patients with AD with severe cognitive performance tend to have a lower GSN level.

#### Plasma GSN level performed a well diagnosis of patients with AD in early stage of the disease duration

Considering the level of GSN might change as AD progressed,<sup>22–24</sup> we further analysed the plasma GSN level by disease course and age at diagnosis stratification. Interestingly, the plasma GSN level was increased in patients with early stage of the disease duration (0–3 years), while it declined in patients with moderate and late stages of the disease duration ( $\geq 4$  years, [figure 4E](#)). The ROC

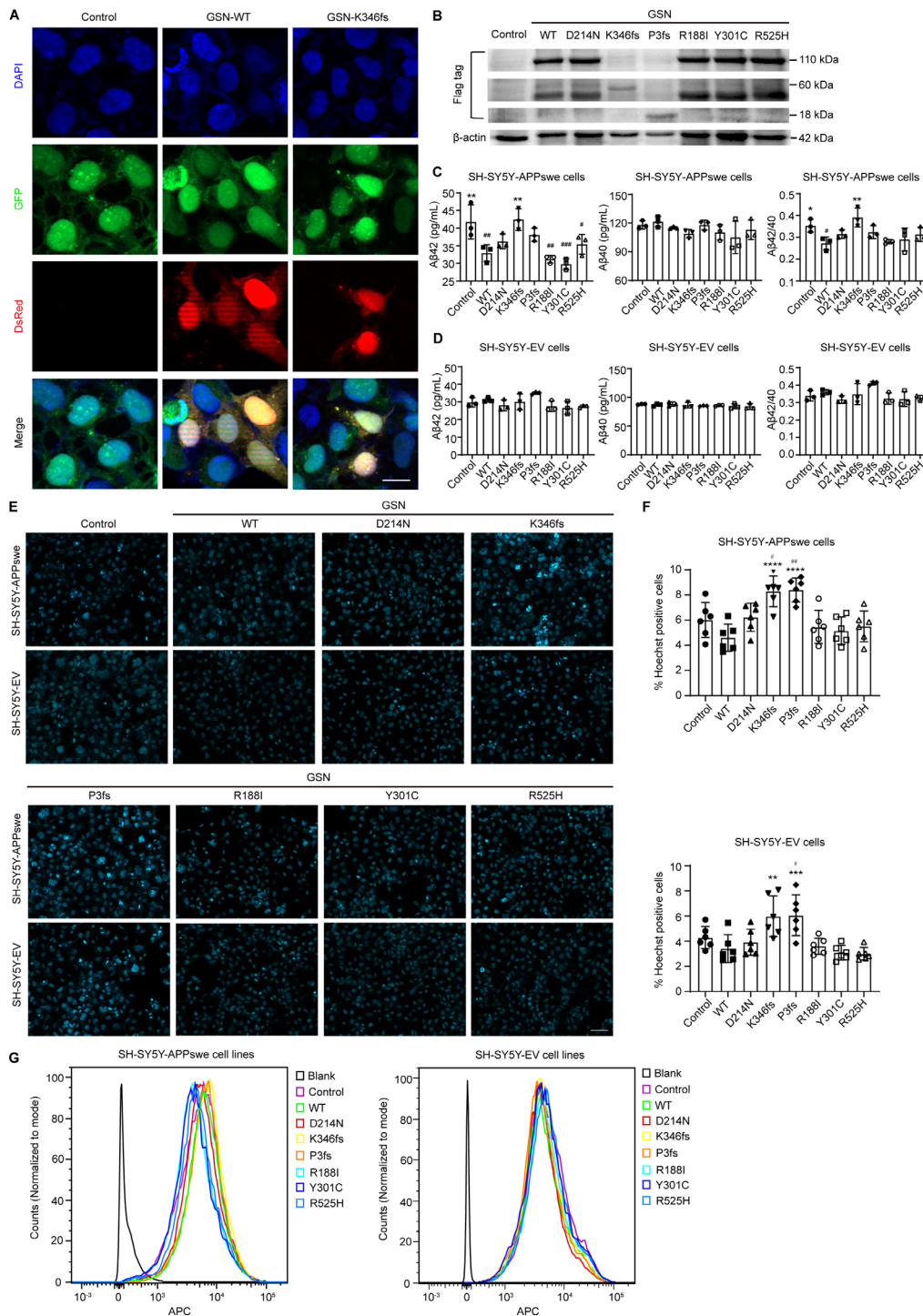


**Figure 2** GSN frameshift mutations failed to reduce the Aβ level and apoptosis in SH-SY5Y-APPsw cells. (A) Immunofluorescence images of SH-SY5Y-APPsw cells transfected with GSN plasmids. SH-SY5Y-APPsw cells were characterised with GFP (green). SH-SY5Y cells transfected with GSN plasmids were characterised with DsRed (red). SH-SY5Y-APPsw cells transfected with GSN plasmids were characterised with both GFP (green) and DsRed (red), which appeared yellow in merged images. Scale bar: 20 μm. (B) Western blot analyses of the flag tag to show the expression of different GSN mutant proteins. GSN-WT was used as the negative control; GSN-D214N was the positive control (reported to be associated with FAF); GSN-K346fs and GSN-P3fs were frameshift mutations identified in patients with AD; GSN-R188I, GSN-Y301C and GSN-R525H were VUS identified in patients with AD and distributed in different domains of GSN (C) GSN K346fs mutation failed to reduce Aβ42 levels or the ratio of Aβ42/40 in SH-SY5Y-APPsw cells, as shown by ELISA analysis. n=3 per group. (D) ELISA analysis of Aβ42 and Aβ40 in SH-SY5Y-EV cells transfected with GSN plasmids. n=3 per group. (E) Immunostaining of Hoechst 33342 (light blue) in SH-SY5Y-APPsw and SH-SY5Y-EV cells transfected with GSN plasmids. Scale bar: 50 μm. (F) Quantification of Hoechst-positive cells in (E). GSN K346fs and P3fs mutations failed to reduce apoptosis in SH-SY5Y-APPsw and SH-SY5Y-EV cells. n=6 per group. (G) ROS levels in SH-SY5Y-APPsw and SH-SY5Y-EV cells transfected with GSN plasmids. #P<0.05 vs the control group, \*P<0.05 vs the WT group, ##\*P<0.05, ###\*\*P<0.01, ####\*\*\*P<0.001, #####\*\*\*\*P<0.0001. Aβ, β-amyloid; AD, Alzheimer's disease; DAPI, 4',6-diamidino-2'-phenylindole; DsRed: discosoma sp. red fluorescent protein; EV, empty lentivirus; FAF, familial amyloidosis of the Finnish type; GFP: green fluorescent protein; GSN, gelsolin; ROS, reactive oxygen species; VUS, variants of undetermined significance; WT, wild type.

J Neurol Neurosurg Psychiatry: first published as 10.1136/jnnp-2022-330465 on 17 January 2023. Downloaded from http://jnnp.bmj.com/ on April 17, 2024 by guest. Protected by copyright.



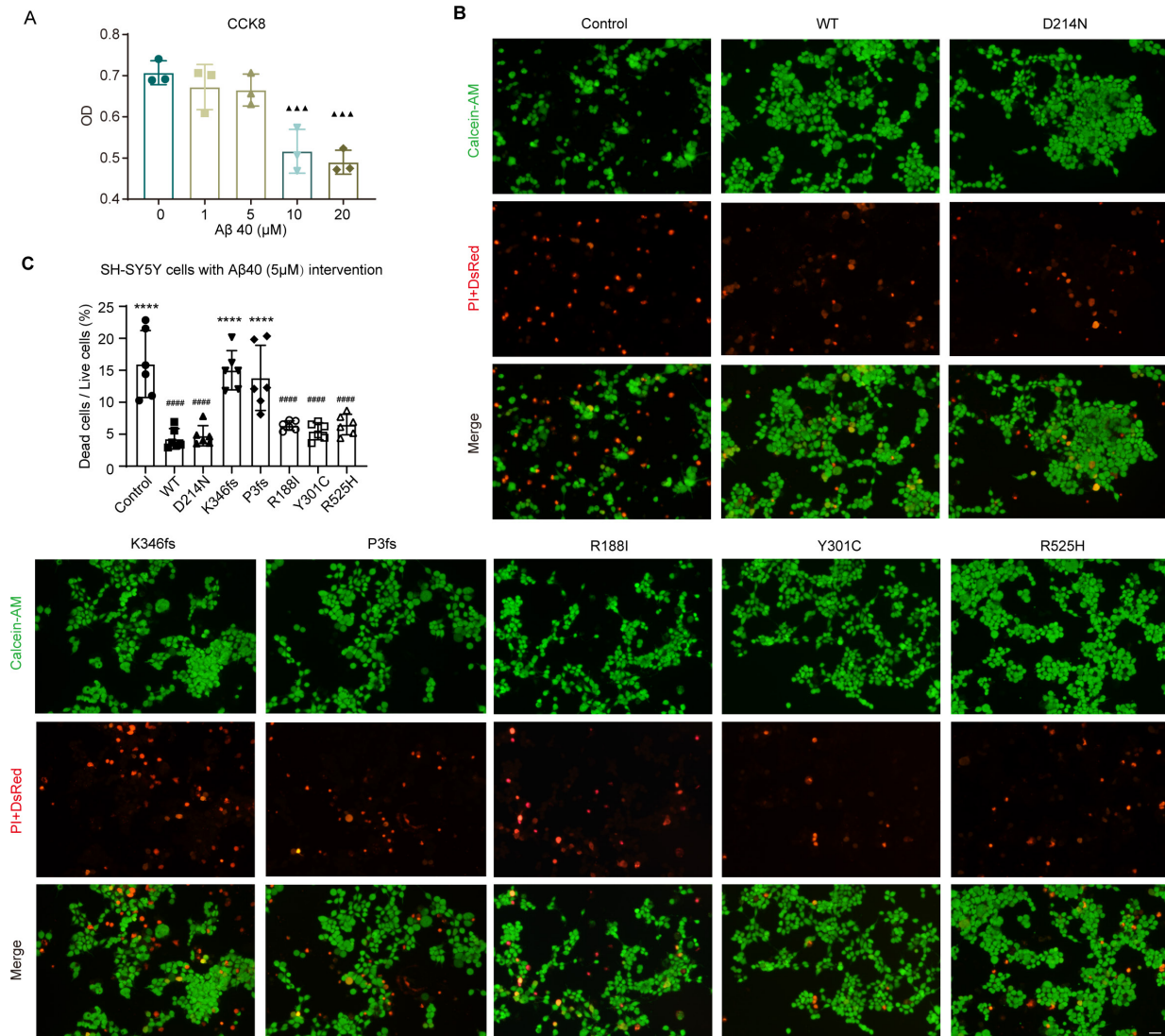


**Figure 3** GSN frameshift mutations failed to inhibit the toxicity of Aβ40 in SH-SY5Y cells. (A) Toxicity analysis of SH-SY5Y cells by CCK8 suggested that the concentration of 5 μM Aβ40 was a suitable concentration for intervention. n=3 per group. (B) Calcein-AM/PI staining images of SH-SY5Y cells transfected with GSN plasmids and then treated with 5 μM Aβ40. Live cells were characterised with calcein-AM (green). Dead cells were characterised with PI (red). Live cells transfected with GSN plasmids appeared yellow in the merged images. Scale bar: 50 μm. (C) Quantification analysis of dead cells in (B). n=6 per group. GSN K346fs and P3fs mutations failed to inhibit the toxicity of Aβ40 in SH-SY5Y cells. ▲p<0.05 vs the 0 μM Aβ40 group, #P<0.05 vs the control group, \*P<0.05 vs the WT group; ▲▲▲P<0.001, #####/\*\*\*\*P<0.0001. GSN, gelsolin; PI, propidium iodide; WT, wild type.

curve revealed a moderate test power to distinguish patients with AD (disease course 0–3 years) from controls (area under curve (AUC)=0.672, p=0.000, cut-off=1.45×10<sup>7</sup> pg/mL; [figure 4F](#)), suggesting that plasma GSN is a potential biomarker at the early stage of AD. Moreover, the plasma GSN level of patients with rather early age was significantly higher than that in controls (61–80 years), which were gradually decreasing with the late age (≥80 years, Online supplemental figure S4A). The ROC curve was analysed between 61 years and 80 years, which also showed a moderate test power to distinguish patients with AD from controls (AUC=0.678, p=0.000, cut-off=1.39×10<sup>7</sup> pg/mL; Online supplemental figure S4B). Additionally, well performance was observed in the ROC curve of GSN frameshift mutations carriers and non-carriers in AD (AUC=0.979, p=0.000, cut-off=7.98×10<sup>6</sup> pg/mL; Online supplemental figure S4C), indicating that the plasma GSN level is able to distinguish patients with AD with GSN frameshift mutations from non-carriers.

### GSN levels were correlated with Aβ pathology and brain atrophy in AD patients

To explore the correlation between the GSN level and AD pathology, CSF AD biomarkers (Aβ42, Aβ40, t-tau and p-tau) were measured using ELISA. The correlation analysis was carried out, and positive correlation between the CSF GSN level and CSF Aβ42 level was observed (r=0.289, p=0.009; [figure 4G](#)). As CSF Aβ42 level were negatively correlated with the Aβ depositions (assessed by global standardized uptake value ratio (SUVR) of Aβ PET),<sup>25</sup> patients with AD with lower CSF GSN level tended to exhibit lower CSF Aβ42 level and more Aβ depositions, while no association existed in CSF GSN and CSF Aβ40, CSF Aβ42/40, CSF t-tau or CSF p-tau ([figure 4H,I](#), and online supplemental figure S5A,B). Besides, the correlation between the plasma GSN and plasma Aβ42 was also analysed, while no significant difference was observed (online supplemental figure S5C).

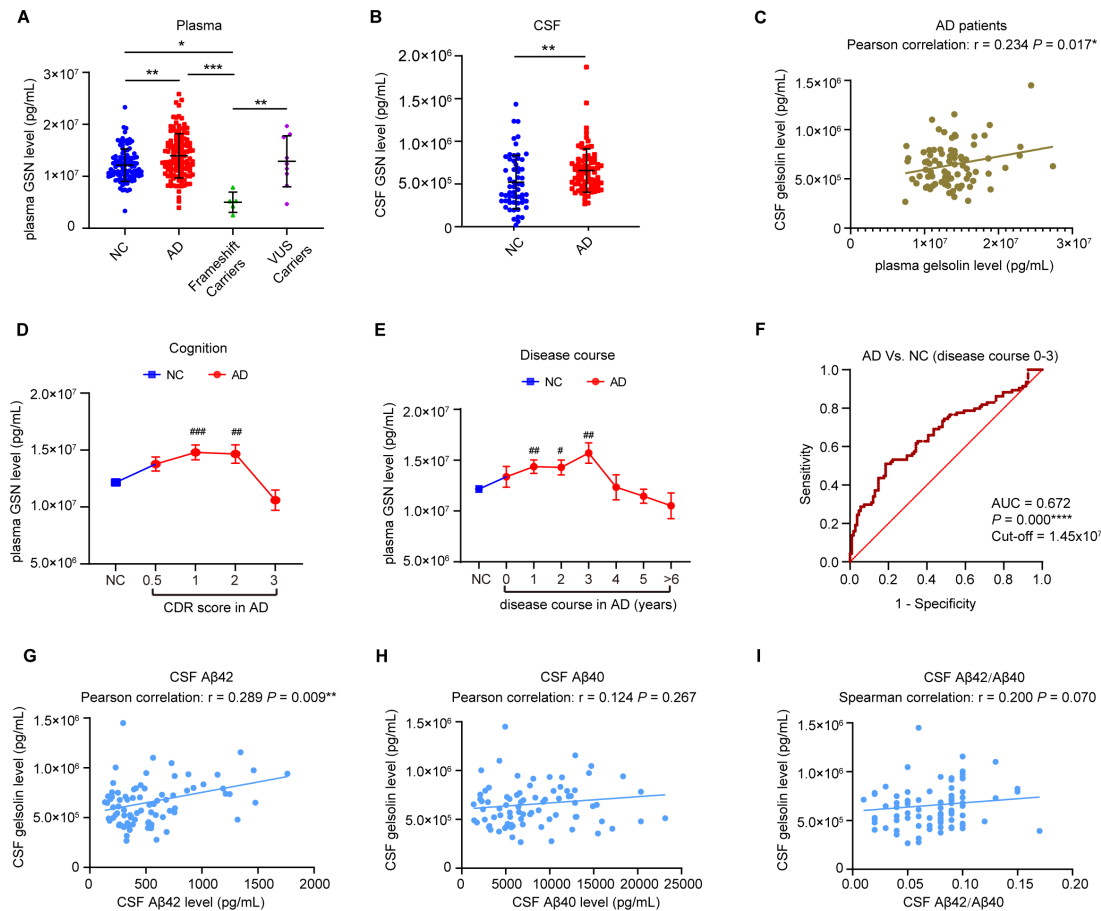


**Figure 4** Plasma GSN levels were significantly higher in patients with AD. (A) Plasma GSN levels in cognitively NCs, patients with AD, *GSN* frameshift mutation carriers and *GSN* VUS carriers by ELISA analysis. Plasma GSN levels in patients with AD were higher than those in NCs, and plasma GSN levels in patients with AD carrying *GSN* frameshift mutations were lower than those in NCs;  $n=124$  in the AD group,  $n=103$  in the NC group,  $n=5$  in the frameshift carrier group and  $n=8$  in the VUS carrier group. (B) CSF GSN levels in cognitively NCs and patients with AD by ELISA analysis. CSF GSN levels in patients with AD were higher than those in NCs;  $n=82$  in the AD group and  $n=59$  in the NC group. (C) The positive correlation between CSF GSN and plasma GSN in patients with AD analysed by Pearson correlation analysis,  $n=82$ . (D) The GSN level changes with CDR score in patients with AD and NC. The plasma GSN level was initially increased in the groups with CDR score=0.5~2, and then reduced in the group with CDR=3. (E) The GSN level changes with disease course in patients with AD and NC. The plasma GSN level was compensatively increased in the disease course between 0 year and 3 years. In contrast, the GSN level was downregulated in the disease course more than 4 years. (F) The ROC curve of plasma GSN levels between patients with AD (disease course 0–3 years) and NC showed a moderate test power to distinguish AD from controls. (G–I) The positive correlation between CSF GSN and CSF A $\beta$ 42, A $\beta$ 40, A $\beta$ 42/A $\beta$ 40 in patients with AD analysed by Pearson or Spearman correlation analysis,  $n=82$ . # $P<0.05$  vs the NC group; \* $P<0.05$ , \*\* $P<0.01$ , \*\*\* $P<0.001$ , \*\*\*\* $P<0.0001$ . AD, Alzheimer's disease; CDR, Clinical Dementia Rating; CSF, cerebrospinal fluid; GSN, gelsolin; NC, normal control; VUS, variants of undetermined significance.

Moreover, the correlation between the GSN level and brain atrophy were analysed, with the increase of global cerebral atrophy-frontal (GCA-F), PA and MTA scores, the plasma or CSF GSN showed a trend of initially increasing and then decreasing (online supplemental figure S6A-F), and the plasma GSN was significantly positively correlated with GCA-F and MTA by Spearman correlation analysis (GCA-F:  $r=0.256$ ,  $p=0.020$ ; MTA:  $r=0.250$ ,  $p=0.038$ ).

## DISCUSSION

To our knowledge, this study was the first to clarify the role of *GSN* frameshift mutations in the pathogenesis of AD, and proposed the genotype–phenotype heterogeneity of the *GSN* gene in which missense mutations lead to FAF, while frameshift mutations cause AD. Besides, the detection of higher plasma GSN levels in patients with AD at an early stage, indicating it possibly would be a potential diagnosis biomarker and monitoring the progression of AD (figure 5).

In this study, we first completed AD and FAF-related examinations in patients with *GSN* frameshift mutations, confirming that patients with *GSN* frameshift mutations were AD phenotype. However, none of the five patients with AD with *GSN* frameshift mutations, reported in the previous study,<sup>8</sup> completed the exclusive FAF diagnosis.<sup>7</sup> Therefore, our present study first demonstrates that frameshift mutations may cause AD phenotype.

Combined with our previous clinical cohort, the frameshift mutations (K346fs and P3fs) of *GSN* could account for 0.5% of AD cases. Moreover, frameshift mutations in the *GSN* gene in patients with AD were only observed in Han populations. Among the reported mutations in the *GSN* gene, there are three frameshift mutations (A34fs, K346fs and P3fs<sup>8 26</sup>), all of which were reported in Han populations, suggesting geographical heterogeneity of the *GSN* mutations. For missense variants, we failed to identify significant enrichment of these missense variants across the *GSN* gene in patients with AD compared with the controls. Interestingly, reported patients with FAF with *GSN* missense

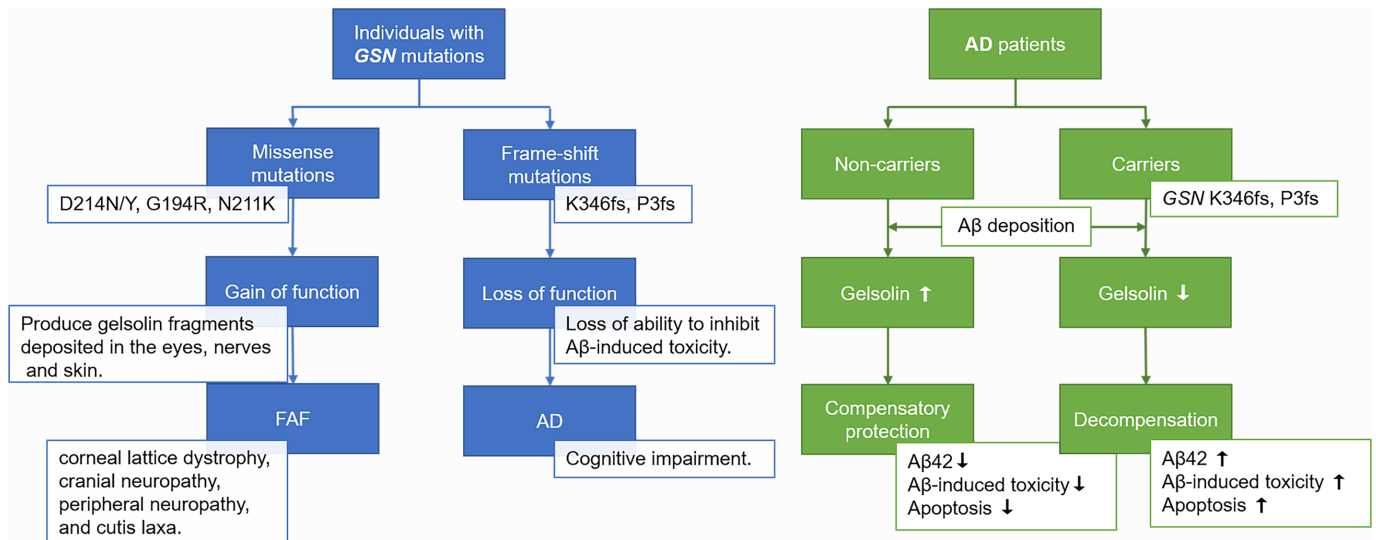


**Figure 5** Schematic diagram. Individuals with different GSN mutations have different clinical phenotypes: missense mutations usually correspond to FAF, while frameshift mutations correspond to AD. Patients with AD who carried GSN frameshift mutations presented extremely low plasma GSN levels, which promoted the progression of AD. Patients with AD without GSN mutations exhibited compensatory increases in plasma GSN levels, which functioned as a protective factor in patients with AD. AD, Alzheimer's disease; FAF, familial amyloidosis of the Finnish type; GSN, gelsolin.

mutations were usually cognitive normal.<sup>7 27–30</sup> Only one study reported that patients with FAF appeared slightly with abnormalities in visuoconstructional and spatial performance,<sup>31</sup> which further confirmed the genotype–phenotype heterogeneity of the GSN gene. The phenomenon of genotype–phenotype heterogeneity has also been reported in other genes previously. Wang *et al*<sup>32</sup> demonstrated that frameshift mutations of *presenilin1* (*PS1*) led to familial acne inversa, which is a dermatological disease. However, pathogenic missense mutations of the *PS1* gene were first reported to cause familial AD.<sup>33</sup> No frameshift mutation was reported as a pathogenic mutation of the *PS1* gene in AD. The different types of mutations of the *PS1* gene contributed to completely different diseases. These studies suggest that different mutational forms of GSN lead to different clinical phenotypes and may be related to the pathogenesis of these diseases.

To figure out that frameshift mutations, rather than missense variants, are involved in AD pathogenesis, we first detected the mRNA and protein levels of GSN and found that the mutant mRNA could not be detected in patients, suggesting that the frameshift mutations did not generate fragments of GSN protein, which might be explained by nonsense-mediated mRNA decay.<sup>34</sup> This was different from the pathogenic process of FAF. As the protein conformation changed in the acknowledged mutations of D214N or N211K,<sup>35 36</sup> GSN could be cleaved when passing through the Golgi, and small fragments were generated during the process. The deposition of fragments on corresponding tissues led to the clinical symptoms of FAF.<sup>37–41</sup> Nevertheless, no fragments were observed in patients with AD with GSN frameshift mutations at the mRNA or protein level. Additionally, we found patients with AD with GSN frameshift mutation had a decreased plasma GSN level, which was not present in patients with AD with identified missense mutations, indicating that the mechanism of loss of function might be involved in the pathogenesis of AD.

Mechanism studies found that GSN contained two A $\beta$  binding sites and could bind and sequester A $\beta$ ,<sup>42</sup> then inhibit A $\beta$  fibrosis and degrade fibres that already formed.<sup>43 44</sup> GSN could also inhibit A $\beta$ -induced cytotoxicity by inhibiting apoptotic mitochondrial changes<sup>45</sup> and protect neurons from apoptosis by actin

remodelling.<sup>46</sup> Then, we selected representative mutation sites and forms to clarify the mechanism of GSN frameshift mutations from the cytological level by observing the A $\beta$ 42 levels and cellular apoptosis in AD model cells transfected with different GSN plasmids. Meaningfully, compared with GSN-WT plasmid treatment, the increased level of A $\beta$ 42, the higher ratio of dead cells:live cells in the A $\beta$ -induced toxicity tests, and more apoptotic cells were observed in the GSN-K346fs and GSN-P3fs plasmid-treated group, suggesting that the K346fs and P3fs mutations lost the protective function of GSN. For groups of missense mutations of GSN, no significant difference was observed, indicating that the mutant protein may retain its function to a certain extent. To our knowledge, the GSN protein can bind A $\beta$ , inhibit its aggregation, and protect cells from apoptosis and ROS.<sup>4 47</sup> Injection or overexpression of GSN resulted in a significant reduction in amyloid loads and a decrease in A $\beta$  levels in AD transgenic mice.<sup>44 48 49</sup> Our results showed that GSN frameshift mutations, rather than identified missense mutations, led to the GSN loss of function in reducing A $\beta$ 42 levels, inhibiting A $\beta$ -induced toxicity, and protecting cells from apoptosis. This was different from the pathogenic process of missense mutations in FAF, which generate small fragments and deposit on tissues of eye, skin and peripheral nerves.<sup>37–41</sup> Thus, different mutational forms of the same gene lead to different pathogenic pathways and present different clinical phenotypes.

Considering that GSN acts as an anti-amyloidogenic protein and might change in AD progression,<sup>4 24</sup> it may be a potential biomarker for AD. However, the plasma GSN levels were inconsistent in patients with AD reported in previous studies.<sup>22 24</sup> In our cohort, the plasma GSN level was higher in early stage of disease duration of AD, and it was lower in medium and late stages of AD than that in controls, suggesting that GSN may function in the compensatory mechanism of the A $\beta$  pathology. As the level of plasma GSN changes as AD progresses, the plasma GSN may be a novel potential biomarker for AD. To further explore the relationship between plasma and CSF GSN level, we also detected GSN level in CSF. The results showed a positive correlation between CSF GSN and plasma GSN, which increased the importance of plasma GSN as a biomarker.



Additionally, the level of plasma GSN in patients with frameshift mutations was significantly decreased, while the level of plasma GSN in patients with missense mutations was comparable to that in controls, further confirming the loss-of-function mechanism of GSN frameshift mutations.

In summary, we found that GSN frameshift mutations are associated with the pathogenesis of AD. The level of GSN increases in the early stage of sporadic AD and has a protective effect, while in patients with frameshift mutations or patients with advanced disease, the level of GSN is downregulated and leads to the development or aggravation of the disease.

#### Author affiliations

<sup>1</sup>Department of Neurology, Xiangya Hospital Central South University, Changsha, Hunan, China

<sup>2</sup>National Clinical Research Center for Geriatric Disorders, Xiangya Hospital Central South University, Changsha, Hunan, China

<sup>3</sup>Engineering Research Center of Hunan Province in Cognitive Impairment Disorders, Xiangya Hospital Central South University, Changsha, Hunan, China

<sup>4</sup>Hunan International Scientific and Technological Cooperation Base of Neurodegenerative and Neurogenetic Diseases, Central South University, Changsha, Hunan, China

<sup>5</sup>Key Laboratory of Hunan Province in Neurodegenerative Disorders, Central South University, Changsha, Hunan, China

<sup>6</sup>Department of Geriatrics Neurology, Xiangya Hospital Central South University, Changsha, Hunan, China

<sup>7</sup>Institute of Molecular Precision Medicine, Key Laboratory of Molecular Precision Medicine of Hunan Province, Xiangya Hospital Central South University, Changsha, Hunan, China

<sup>8</sup>Center for Medical Genetics, School of Life Sciences, Central South University, Changsha, Hunan, China

<sup>9</sup>Key Laboratory of Organ Injury, Aging and Regenerative Medicine of Hunan Province, Xiangya Hospital, Changsha, Hunan, China

**Acknowledgements** We thank the CIMDCNC and ADSP database for supporting our study.

**Contributors** LS, BJ and YJ conceived the project and designed the experiments. YJ, MW, XX, ZL, XL, HZ, LZ and JL (Jingyi Lin) performed the experiments. LS, BJ, YZ, XL, LW, JW, JG, HJ, ZZ, KX, JL (Jiada Li) and BT performed the technical consultation. YJ, MW and XL contributed to the data acquisition and analysis. LS, YJ and BJ wrote the manuscript. All authors reviewed and revised the manuscript. LS and BJ, acting as guarantors, are responsible for the overall content of the study.

**Funding** This study was supported the National Key R&D Program of China (number 2020YFC2008500), the National Major Projects in Brain Science and Brain-like Research (number 2021ZD0201803), the National Natural Science Foundation of China (number 81971029, 82071216 and 81901171), Hunan Innovative Province Construction Project (number 2019SK2335) and Hu-Xiang Youth Project (number 2021RC3028).

**Competing interests** None declared.

**Patient consent for publication** Consent obtained directly from patient(s).

**Ethics approval** This study involves human participants and was approved by the ethics committee of Xiangya Hospital, Central South University (institutional review board equivalent, reference number 2019030501). Written informed consent was obtained from all participants involved in the study.

**Provenance and peer review** Not commissioned; externally peer reviewed.

**Data availability statement** Data are available upon reasonable request. All data relevant to the study are included in the article or uploaded as supplementary information.

**Supplemental material** This content has been supplied by the author(s). It has not been vetted by BMJ Publishing Group Limited (BMJ) and may not have been peer-reviewed. Any opinions or recommendations discussed are solely those of the author(s) and are not endorsed by BMJ. BMJ disclaims all liability and responsibility arising from any reliance placed on the content. Where the content includes any translated material, BMJ does not warrant the accuracy and reliability of the translations (including but not limited to local regulations, clinical guidelines, terminology, drug names and drug dosages), and is not responsible for any error and/or omissions arising from translation and adaptation or otherwise.

**Open access** This is an open access article distributed in accordance with the Creative Commons Attribution Non Commercial (CC BY-NC 4.0) license, which permits others to distribute, remix, adapt, build upon this work non-commercially, and license their derivative works on different terms, provided the original work is

properly cited, appropriate credit is given, any changes made indicated, and the use is non-commercial. See: <http://creativecommons.org/licenses/by-nc/4.0/>.

#### ORCID iDs

Junling Wang <http://orcid.org/0000-0001-5117-5204>

Jifeng Guo <http://orcid.org/0000-0002-3658-3928>

Hong Jiang <http://orcid.org/0000-0002-7646-5950>

Lu Shen <http://orcid.org/0000-0002-3393-8578>

#### REFERENCES

- Knopman DS, Amieva H, Petersen RC, *et al.* Alzheimer disease. *Nat Rev Dis Primers* 2021;7:33.
- Lane CA, Hardy J, Schott JM. Alzheimer's disease. *European Journal of Neurology* 2018;25:59–70.
- Tiwari S, Atluri V, Kaushik A, *et al.* Diagnostics, and therapeutics. *Int J Nanomedicine* 2019;14:5541–54.
- Feldt J, Schicht M, Garreis F, *et al.* Structure, regulation and related diseases of the actin-binding protein gelsolin. *Expert Rev Mol Med* 2018;20:e7.
- Yu Y, Sun X, Tang D, *et al.* Gelsolin bound  $\beta$ -amyloid peptides (1–40/1–42) : Electrochemical evaluation of levels of soluble peptide associated with Alzheimer's disease. *Biosensors and Bioelectronics* 2015;68:115–21.
- Ji L, Zhao X, Hua Z. Potential therapeutic implications of gelsolin in Alzheimer's disease. *Journal of Alzheimer's Disease* 2015;44:13–25.
- Nikoskinen T, Schmidt E-K, Strbian D, *et al.* Natural course of Finnish gelsolin amyloidosis. *Ann Med* 2015;47:506–11.
- Jiang Y, Jiao B, Liao X, *et al.* Analyses Mutations in GSN, CST3, TTR, and ITM2B Genes in Chinese Patients With Alzheimer's Disease. *Front Aging Neurosci* 2020;12:581524.
- Sperling RA, Aisen PS, Beckett LA, *et al.* Toward defining the preclinical stages of Alzheimer's disease: Recommendations from the National Institute on Aging-Alzheimer's Association workgroups on diagnostic guidelines for Alzheimer's disease. *Alzheimer's & Dementia* 2011;7:280–92.
- Crane PK, Foroud T, Montine TJ, *et al.* Alzheimer's Disease Sequencing Project discovery and replication criteria for cases and controls: Data from a community-based prospective cohort study with autopsy follow-up. *Alzheimer's & Dementia* 2017;13:1410–3.
- Beecham GW, Bis JC, Martin ER, *et al.* The Alzheimer's Disease Sequencing Project: Study design and sample selection. *Neurology Genetics* 2017;3:e194.
- Zhang X, Farrell JJ, Tong T, *et al.* Association of mitochondrial variants and haplogroups identified by whole exome sequencing with Alzheimer's disease. *Alzheimers Dement* 2022;18:294–306.
- Jack CR, Bennett DA, Blennow K, *et al.* NIA-AA Research Framework: Toward a biological definition of Alzheimer's disease. *Alzheimer's & Dementia* 2018;14:535–62.
- Li J, Zhao T, Zhang Y, *et al.* Performance evaluation of pathogenicity-computation methods for missense variants. *Nucleic Acids Res* 2018;46:7793–804.
- Seeburger JL, Holder DJ, Combrinck M, *et al.* Cerebrospinal Fluid Biomarkers Distinguish Postmortem-Confirmed Alzheimer's Disease from Other Dementias and Healthy Controls in the OPTIMA Cohort. *Journal of Alzheimer's Disease* 2015;44:525–39.
- Haass C, Lemere CA, Capell A, *et al.* The Swedish mutation causes early-onset Alzheimer's disease by  $\beta$ -secretase cleavage within the secretory pathway. *Nat Med* 1995;1:1291–6.
- Crowley LC, Marfell BJ, Waterhouse NJ. Analyzing cell death by nuclear staining with Hoechst 33342. *Cold Spring Harb Protoc* 2016;2016.pdb.prot087205.
- Yin H, Zhou M, Chen X, *et al.* Fructose-coated Ångstrom silver prevents sepsis by killing bacteria and attenuating bacterial toxin-induced injuries. *Theranostics* 2021;11:8152–71.
- Zhang D-F, Fan Y, Xu M, *et al.* Complement C7 is a novel risk gene for Alzheimer's disease in Han Chinese. *Natl Sci Rev* 2019;6:257–74.
- Asahina A, Yokoyama T, Ueda M, *et al.* Hereditary gelsolin amyloidosis: a new Japanese case with cutis laxa as a diagnostic clue. *Acta Derm Venereol* 2011;91:201–3.
- Makioka K, Ikeda M, Ikeda Y, *et al.* Familial amyloid polyneuropathy (Finnish type) presenting multiple cranial nerve deficits with carpal tunnel syndrome and orthostatic hypotension. *Neurol Res* 2010;32:472–5.
- Yao F, Zhang K, Zhang Y, *et al.* Identification of Blood Biomarkers for Alzheimer's Disease Through Computational Prediction and Experimental Validation. *Front Neurol* 2018;9:1158.
- Peng M, Jia J, Qin W. Plasma gelsolin and matrix metalloproteinase 3 as potential biomarkers for Alzheimer disease. *Neurosci Lett* 2015;595:116–21.
- Güntert A, Campbell J, Saleem M, *et al.* Plasma gelsolin is decreased and correlates with rate of decline in Alzheimer's disease. *Journal of Alzheimer's Disease* 2010;21:585–96.
- Xie Q, Ni M, Gao F, *et al.* Correlation between cerebrospinal fluid core Alzheimer's disease biomarkers and  $\beta$ -amyloid PET in Chinese dementia population. *ACS Chem Neurosci* 2022;13:1558–65.

- 26 Feng X, Zhu H, Zhao T, *et al.* A new heterozygous G duplicate in exon1 (c.100dupG) of *gelsolin* gene causes Finnish *gelsolin* amyloidosis in a Chinese family. *Brain Behav* 2018;8:e01151.
- 27 Mustonen T, Holkeri A, Holmström M, *et al.* Cardiac manifestations in Finnish *gelsolin* amyloidosis patients. *Amyloid* 2021;28:168–72.
- 28 Cabral-Macias J, Garcia-Montaño LA, Pérezpeña-Díazconti M, *et al.* Clinical, histopathological, and in silico pathogenicity analyses in a pedigree with familial amyloidosis of the Finnish type (Meretoja syndrome) caused by a novel *gelsolin* mutation. *Mol Vis* 2020;26:345–54.
- 29 Taira M, Ishiura H, Mitsui J, *et al.* Clinical features and haplotype analysis of newly identified Japanese patients with *gelsolin*-related familial amyloidosis of Finnish type. *Neurogenetics* 2012;13:237–43.
- 30 Lüttmann RJ, Teismann I, Husstedt IW, *et al.* Hereditary amyloidosis of the Finnish type in a German family: clinical and electrophysiological presentation. *Muscle Nerve* 2010;41:NA–84.
- 31 Kantanen M, Kiuru-Enari S, Salonen O, *et al.* Subtle neuropsychiatric and neurocognitive changes in hereditary *gelsolin* amyloidosis (AGel amyloidosis). *PeerJ* 2014;2:e493.
- 32 Wang B, Yang W, Wen W, *et al.*  $\gamma$ -Secretase Gene Mutations in Familial Acne Inversa. *Science* 2010;330:1065.
- 33 Citron M, Westaway D, Xia W, *et al.* Mutant presenilins of Alzheimer's disease increase production of 42-residue amyloid  $\beta$ -protein in both transfected cells and transgenic mice. *Nat Med* 1997;3:67–72.
- 34 Karousis ED, Mühlemann O. Nonsense-Mediated mRNA decay begins where translation ends. *Cold Spring Harb Perspect Biol* 2019;11:a032862.
- 35 Mustonen T, Schmidt E-K, Valori M, *et al.* Common origin of the *gelsolin* gene variant in 62 Finnish AGel amyloidosis families. *European Journal of Human Genetics* 2018;26:117–23.
- 36 Efebera YA, Sturm A, Baack EC, *et al.* Novel *gelsolin* variant as the cause of nephrotic syndrome and renal amyloidosis in a large kindred. *Amyloid* 2014;21:110–2.
- 37 Zorgati H, Larsson M, Ren W, *et al.* The role of *gelsolin* domain 3 in familial amyloidosis (Finnish type). *Proc Natl Acad Sci U S A* 2019;116:13958–63.
- 38 Giorgino T, Mattioni D, Hassan A, *et al.* Nanobody interaction unveils structure, dynamics and proteotoxicity of the Finnish-type amyloidogenic *gelsolin* variant. *Biochim Biophys Acta Mol Basis Dis* 2019;1865:648–60.
- 39 Boni F, Milani M, Porcari R, *et al.* Molecular basis of a novel renal amyloidosis due to N184K *gelsolin* variant. *Sci Rep* 2016;6:33463.
- 40 Kazmirski SL, Isaacson RL, An C, *et al.* Loss of a metal-binding site in *gelsolin* leads to familial amyloidosis–Finnish type. *Nat Struct Biol* 2002;9:112–6.
- 41 Chen C-D *et al.* Furin initiates *gelsolin* familial amyloidosis in the Golgi through a defect in Ca<sup>2+</sup> stabilization. *Embo J* 2001;20:6277–87.
- 42 Chauhan VPS, Ray I, Chauhan A, *et al.* Binding of *gelsolin*, a secretory protein, to amyloid  $\beta$ -protein. *Biochem Biophys Res Commun* 1999;258:241–6.
- 43 Ray I, Chauhan A, Wegiel J, *et al.* *Gelsolin* inhibits the fibrillization of amyloid beta-protein, and also defibrillizes its preformed fibrils. *Brain Res* 2000;853:344–51.
- 44 Hirko AC, Meyer EM, King MA, *et al.* Peripheral Transgene Expression of Plasma *Gelsolin* Reduces Amyloid in Transgenic Mouse Models of Alzheimer's Disease. *Molecular Therapy* 2007;15:1623–9.
- 45 Qiao H, Koya RC, Nakagawa K, *et al.* Inhibition of Alzheimer's amyloid- $\beta$  peptide-induced reduction of mitochondrial membrane potential and neurotoxicity by *gelsolin*. *Neurobiol Aging* 2005;26:849–55.
- 46 Harms C, Bösel J, Lautenschlager M, *et al.* Neuronal *gelsolin* prevents apoptosis by enhancing actin depolymerization. *Molecular and Cellular Neuroscience* 2004;25:69–82.
- 47 Kothakota S, Azuma T, Reinhard C, *et al.* Caspase-3-generated fragment of *gelsolin*: effector of morphological change in apoptosis. *Science* 1997;278:294–8.
- 48 Yang W, Chauhan A, Mehta S, *et al.* Trichostatin A increases the levels of plasma *gelsolin* and amyloid beta-protein in a transgenic mouse model of Alzheimer's disease. *Life Sci* 2014;99:31–6.
- 49 Antequera D, Vargas T, Ugalde C, *et al.* Cytoplasmic *gelsolin* increases mitochondrial activity and reduces A $\beta$  burden in a mouse model of Alzheimer's disease. *Neurobiol Dis* 2009;36:42–50.

## ***GSN* Gene Frameshift Mutations in Alzheimer's Disease**

Yaling Jiang, Meidan Wan, Xuewen Xiao, Zhuojie Lin, Xixi Liu, Yafang Zhou, Xinxin Liao, Jingyi Lin, Hui Zhou, Lu Zhou, Ling Weng, Junling Wang, Jifeng Guo, Hong Jiang, Zhuohua Zhang, Kun Xia, Jiada Li, Beisha Tang, Bin Jiao\*, Lu Shen\*

### **Include:**

**Supplementary methods**

**Supplementary Figure S1-6**

**Supplementary Table S1**

### **Supplementary methods**

#### **ATN framework diagnosis classification**

The  $\beta$  amyloid deposition, pathologic tau, and neurodegeneration (ATN) framework[1] was described below:  $A\beta_{42}$  level in CSF  $< 651$  pg/ml, or  $A\beta_{42}/A\beta_{40}$  ratio  $\leq 0.1$ , is defined as positive amyloidosis (corresponding to A+ in the ATN framework); p-tau  $> 61$  pg/ml in CSF is defined as neurofibrillary tangles (corresponding to T+ in the ATN framework); t-tau  $\geq 290$  pg/ml in CSF is defined as nerve cell death (corresponding to N+ in the ATN framework).

#### **Cognitive Impairment Multicenter Database and Collaborative Network in China (CI-MDCNC)**

The CI-MDCNC cohort recruited 884 AD patients from 8 clinical sites across China, which is one of the largest multicenter, observational, longitudinal, and natural history studies of AD in China.

#### **Alzheimer's Disease Sequencing Project (ADSP) public database**

The ADSP performed whole exome sequencing (WES) of DNA specimens obtained from 5,778 AD cases and 5,136 controls, including 5,519 AD cases and 4,917



cognitively normal elderly controls of European ancestry (EA) and 218 AD cases and 177 controls of Caribbean Hispanic (CH) heritage[2-4].

### **Targeted gene sequencing**

The targeted gene sequencing panel includes four genes (GSN, APP, PSEN1, and PSEN2). The specific methods were described previously[5]. In brief, the genomic DNA was broken into 200-250 bp length fragments by Covaris LE220 (MA, USA). End-repairing, A-tailing, adaptor ligation, and a 15-cycle pre-capture PCR amplification were performed in fragmented DNA. The products were captured by the targeted gene sequencing panel and sequenced on Illumina HiSeq X Ten Analyzers (Illumina, San Diego, CA, USA) after quality control. Then, the bioinformatics processing and data analysis were performed.

### **3D model structure**

The three-dimensional (3D) models of the mutant protein structures were built by Discovery Studio software. We used homology models of gelsolin in the Protein Data Bank (PDB; No. 3ffn) to construct the 3D structure of the mutant proteins by Discovery Studio software. The known 3D model of the GSN D214N mutant protein was from the PDB (No. 6qbf).

### **Global cerebral atrophy-frontal sub-scale (GCA-F)**

The GCA-F scale is defined in the frontal cortex and sulcal. It ranks 0 to 3, with grade 0 representing no cortical atrophy; grade 1, mild atrophy (dilatation of sulci); grade 2, moderate atrophy (loss of gyri volume); and grade 3, end-stage “knife blade atrophy”.[6, 7]

### **Posterior atrophy (PA)**

The PA scale is defined in the posterior cingulate sulcus, parieto-occipital sulcus, precuneus, and parietal cortex. It ranks atrophy from 0 to 3, with grade 0 showing no cortical atrophy; grade 1, mild parietal cortical atrophy, with mild enlargement of the posterior cingulate and parieto-occipital sulcus; grade 2, substantial parietal atrophy, with substantial enlargement of the posterior cingulate and parieto-occipital sulcus; grade 3, end-stage “knife-blade” atrophy, with extreme enlargement of the posterior cingulate and parieto-occipital sulcus.[8]

### **Medial temporal lobe atrophy (MTA)**

The MTA scale is defined in the hippocampus, parahippocampal gyrus, and surrounding CSF spaces. It ranks the degree of MTA from 0 to 4, with grade 0 denoting no cortical atrophy; grade 1, enlargement of choroid fissure; grade 2, along with enlargement of the temporal horn of the lateral ventricle; grade 3, moderate loss of hippocampal volume; and grade 4, severe loss of hippocampal volume.[9]

### **Reference:**

1. Jack CR, Jr., Bennett DA, Blennow K, Carrillo MC, Dunn B, Haeberlein SB, et al. NIA-AA Research Framework: Toward a biological definition of Alzheimer's disease. *Alzheimer's & dementia : the journal of the Alzheimer's Association*. 2018;14(4):535-62.
2. Crane P, Foroud T, Montine T, Larson E. Alzheimer's Disease Sequencing Project discovery and replication criteria for cases and controls: Data from a community-based prospective cohort study with autopsy follow-up. *Alzheimer's & dementia : the journal of the Alzheimer's Association*. 2017;13(12):1410-3.
3. Beecham GW, Bis JC, Martin ER, Choi SH, DeStefano AL, van Duijn CM, et al. The Alzheimer's Disease Sequencing Project: Study design and sample selection. *Neurology Genetics*. 2017;3(5):e194.
4. Zhang X, Farrell J, Tong T, Hu J, Zhu C, Wang L, et al. Association of mitochondrial variants and haplogroups identified by whole exome sequencing with Alzheimer's disease. *Alzheimer's & dementia : the journal of the Alzheimer's Association*. 2021.
5. Jiang Y, Jiao B, Liao X, Xiao X, Liu X, Shen L. Analyses Mutations in GSN, CST3, TTR, and ITM2B Genes in Chinese Patients With Alzheimer's Disease. *Frontiers in aging neuroscience*. 2020;12:581524.
6. Zhu H, Lu H, Wang F, Liu S, Shi Z, Gan J, et al. Characteristics of Cortical Atrophy and White Matter Lesions Between Dementia With Lewy Bodies and Alzheimer's Disease: A Case-Control Study. *Frontiers in neurology*. 2021;12:779344.
7. Wan MD, Liu H, Liu XX, Zhang WW, Xiao XW, Zhang SZ, et al. Associations of

multiple visual rating scales based on structural magnetic resonance imaging with disease severity and cerebrospinal fluid biomarkers in patients with Alzheimer's disease. *Frontiers in aging neuroscience*. 2022;14:906519.

8. Koedam EL, Lehmann M, van der Flier WM, Scheltens P, Pijnenburg YA, Fox N, et al. Visual assessment of posterior atrophy development of a MRI rating scale. *European radiology*. 2011;21(12):2618-25.

9. Scheltens P, Leys D, Barkhof F, Huglo D, Weinstein HC, Vermersch P, et al. Atrophy of medial temporal lobes on MRI in "probable" Alzheimer's disease and normal ageing: diagnostic value and neuropsychological correlates. *Journal of neurology, neurosurgery, and psychiatry*. 1992;55(10):967-72.



## Supplementary Figure S1-6

A

Gene	Primer sequence	Annealing temperature	Size
GSN-K346fs	Forward 5'-AGCTGGCCAAGCTCTACAAG-3'	60 °C	181 bp
	Reverse 5'-TTCCTCTCCTCCGTGTTTGC-3'		
GSN-P3fs	Forward 5'-ACTTAAGGTCGGCGACCC-3'	56 °C	454 bp (Mut)
	Reverse 5'-CGTTCAGGTAGTCATCCAGC-3'		482 bp (WT)
GAPDH	Forward 5'-AGTTAAAAGCAGCCCTGGTGA-3'	60 °C	131 bp
	Reverse 5'-TCGACAGTCAGCCGCATCT-3'		

B GSN-K346fs cDNA sequencing

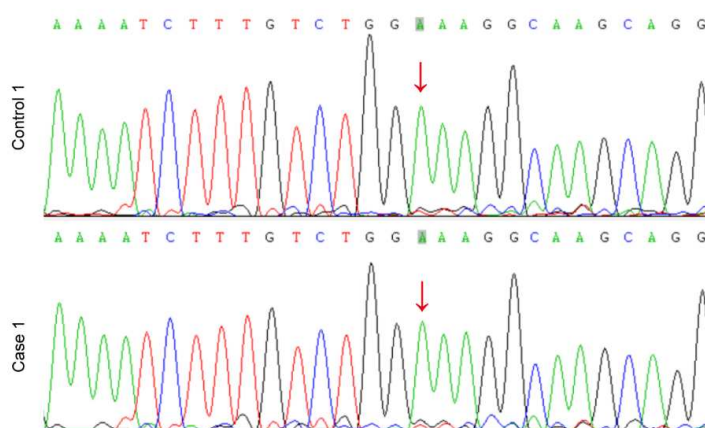


**Figure S1** PCR primers and cDNA sequences. **(A)** The PCR primers for GSN frameshift mutations. **(B)** The cDNA sequencing of Case 1 with the K346fs mutation was the same as that of Control 1.

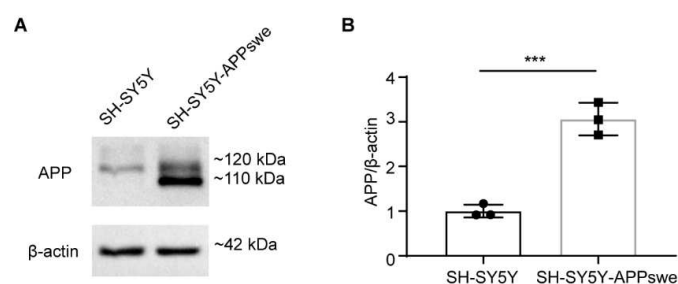


**Figure S2** Identification of AD model cells. **(A-B)** Representative western blot **(A)** and quantification **(B)** of APP expression in SH-SY5Y and SH-SY5Y-APPswe cells. SH-SY5Y-APPswe cells expressed more APP proteins. \*\*\*  $P < 0.001$ .

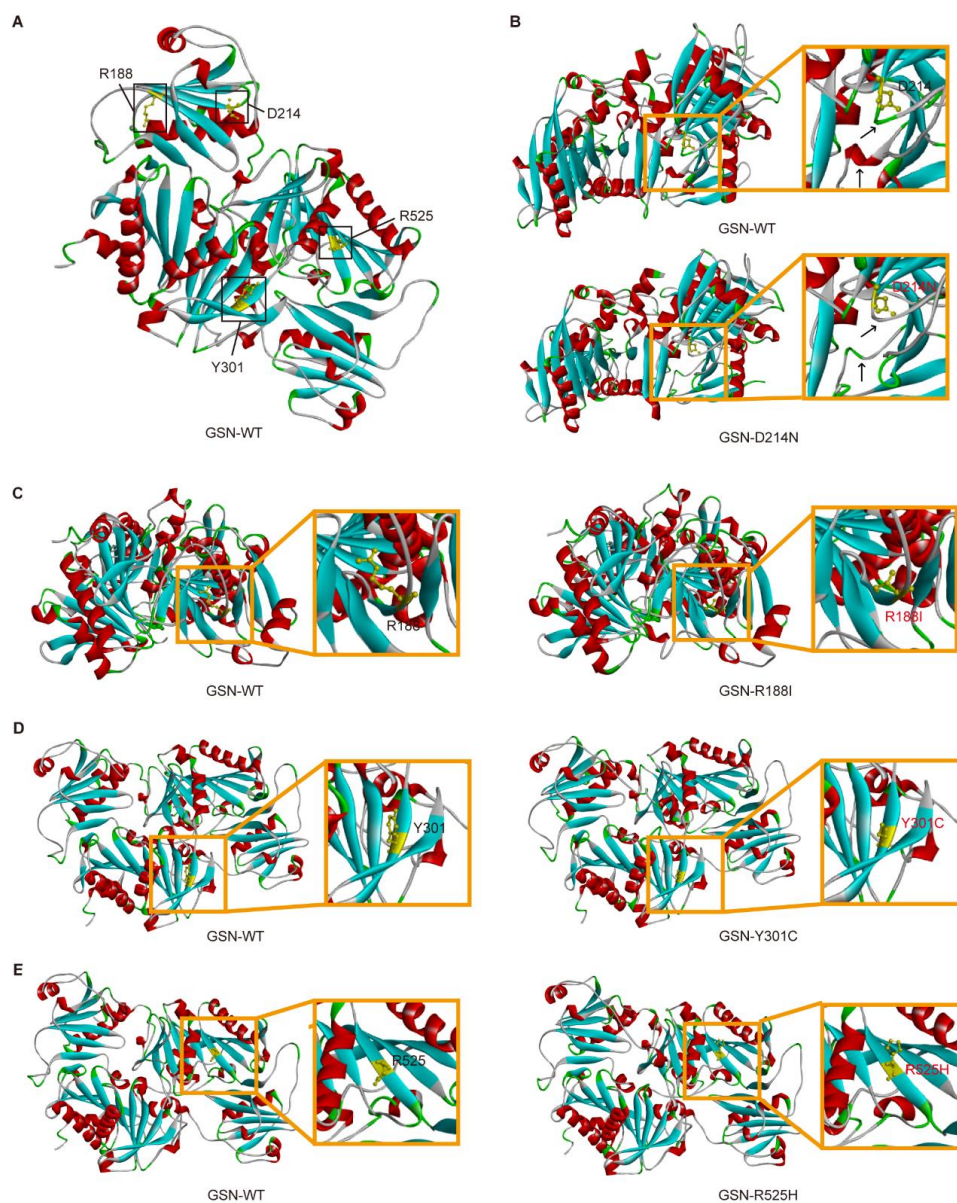


**Figure S3** The 3D model of mutant gelsolin proteins. (A) The 3D model of human gelsolin wild type (GNS-WT) from the Protein Data Bank (No. 3ffn). (B) The different 3D configurations between GNS-WT and GNS D214N mutant proteins. The arrows indicate the difference in protein structures between WT and mutant proteins. The different colours of proteins represent different secondary types of proteins. Amino acids of interest are marked in yellow. The orange square indicates the amplification regions. (C-E) Similar 3D configurations between GNS-WT and GNS mutant proteins (D214N (B), R188I (C), Y301C (D), and R525H (E)).

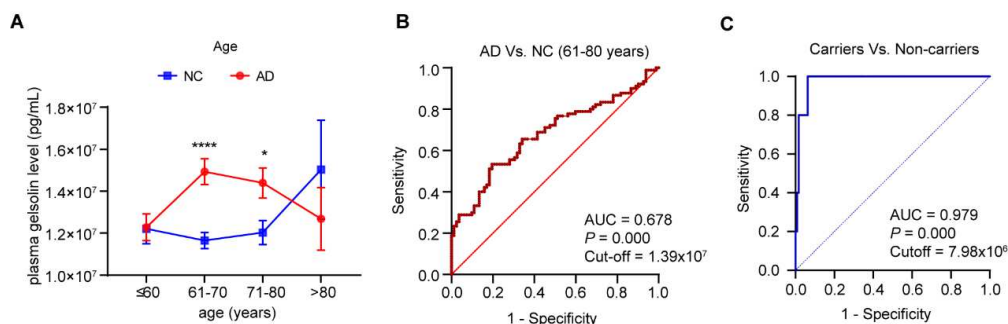


**Figure S4** (A) The gelsolin level changes with age in AD patients and NC. The plasma gelsolin level was compensatively increased in the age between 61 to 80 years. In contrast, the gelsolin level was lower than that in the control in the stage more than 80 years. (B) The ROC curve of plasma gelsolin levels between AD patients and NC (age 61-80 years) showed a moderate test power to distinguish AD from controls. (C) The ROC curve of plasma gelsolin levels between AD patients with *GSN* frameshift mutation carriers and noncarriers showed good test power to distinguish carriers from noncarriers. \*  $P < 0.05$  versus the NC group, and \*\*\*\*  $P < 0.001$ .

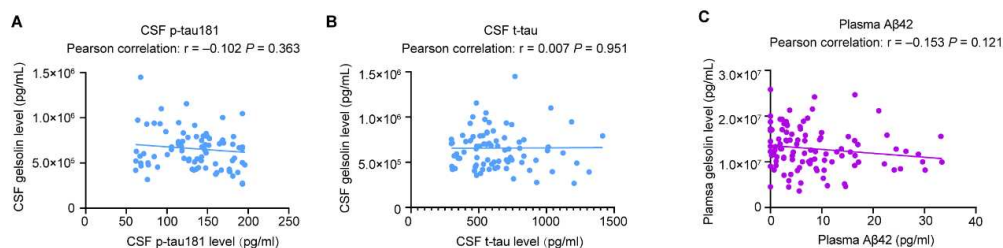


**Figure S5** (A) The negative correlation between CSF gelsolin and CSF p-tau181 in AD patients analyzed by Pearson correlation analysis.  $n = 82$ . (B) The positive correlation between CSF gelsolin and CSF t-tau in AD patients analyzed by Pearson correlation analysis.  $n = 82$ . (C) The negative correlation between plasma gelsolin and plasma Aβ42 in AD patients analyzed by Pearson correlation analysis.  $n = 124$ .

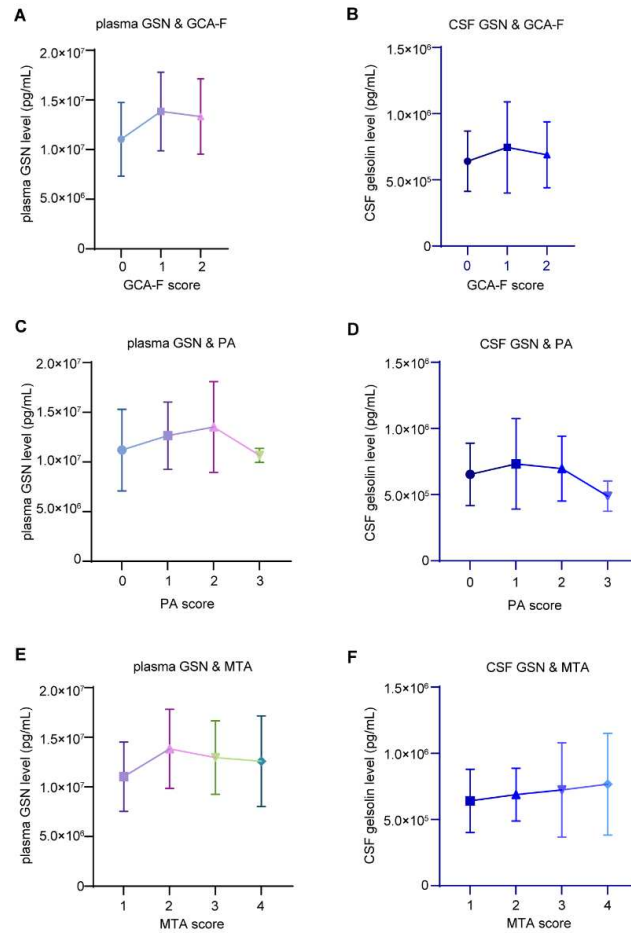


**Figure S6** The relationship between gelsolin and brain atrophy. **(A-B)** The gelsolin level (plasma **(A)** and CSF **(B)**) changes with GCA-F scores in AD patients. **(C-D)** The gelsolin level (plasma **(C)** and CSF **(D)**) changes with PA scores in AD patients. **(E-F)** The gelsolin level (plasma **(E)** and CSF **(F)**) changes with MTA scores in AD patients.

## Supplementary Table

Table S1 Frameshift mutations of the *GSN* gene in the CI-MDCNC cohort

AA Change	SNP	Mutation type	gnomAD_exome_ALL	gnomAD_exome_EAS	ExAC_ALL	ExAC_EAS	Reve	Functional predictions: pathogenic (total)	Patients	Controls
<b>Frameshift mutations</b>										
exon1:c.8_35del:p.P3fs	rs764841269	Frameshift	0	0	0	0	NA	NA	10	0
exon10:c.1408delG;p.G470fs	rs758669795	Frameshift	4.06E-06	5.79E-05	8.24E-06	1.00E-04	NA	NA	1	0
exon12:c.1655dupC;p.S552fs	rs769989772	Frameshift	1.25E-05	2.00E-04	1.91E-05	3.00E-04	NA	NA	2	0
Carriers (n)									13	0
Frequency (%)									1.47% (13/884)	0.00% (0/1403)
<b>P value</b>									<b>&lt;0.001***</b>	